EUROPEAN ORGANIZATION FOR NUCLEAR RESEARCH

A PLASTIC SCINTILLATION SPECTROMETER FOR HIGH-ENERGY BETA PARTICLES

Eberhard Beck

CERN, Geneva, Switzerland*)

ABSTRACT

A scintillation spectrometer has been built to measure beta spectra of short-lived isotopes. The spectrometer consists of two scintillators working in coincidence. The equipment has been calibrated for both electrons and positrons up to 9 MeV using the external beam of a betatron. The resolution ΔE of the spectrometer was found to vary with energy E as $\Delta E \propto E^{1/2}$. The pile-up of positron pulses with pulses from Compton recoil electrons of the annihilation radiation created in the scintillator was studied in detail. Its influence on the positron end-point energy was found to be small. In order to test the spectrometer, maximum beta energies in the decay of ^{68}Ga, ^{82}Rb, ^{90}Y, ^{106}Rh, and ^{118}I have been determined.

Geneva - 30 May 1969

(Submitted to Nuclear Instrum. Methods)

---

*) On leave from the Max-Planck-Institut für Kernphysik, Heidelberg

1. INTRODUCTION

A quantity of fundamental interest in nuclear physics is the Q-value, i.e. the energy difference between ground states of neighbouring isobars. If the nuclide of interest decays by electron or positron emission, the Q-value can be obtained by measuring the maximum beta energy, provided the transition leads to the ground state of the daughter nucleus. In other cases, beta-gamma coincidences can give information about the maximum decay energy available. The spectrometer that will be described in this article was assembled to measure on-line the beta spectra of short-lived isotopically pure sources, produced by the ISOLDE facility[1)]. Because of the short half-lives of the nuclides of interest (a few seconds or minutes) and because of the low activity obtained for nuclei far off the stability line, a plastic scintillation spectrometer was chosen rather than a magnetic spectrometer. The main advantage of the scintillation spectrometer arises from the ability to measure the complete beta-ray continuum simultaneously. On the other hand, the spectra recorded with the scintillation spectrometer are distorted by the finite energy resolution, the electron back-scattering at the scintillator surface, the background from gamma radiation and, in the case of positron decay, the summing up of the positron pulses with those from Compton recoil electrons of annihilation radiation created in the scintillator (in the following referred to as pile-up). Therefore the measured spectra have to be corrected for these distortion effects.

2. EXPERIMENTAL SET-UP

The spectrometer, which is of the same type as the one used by Amarel et al.[2)], consists of two scintillators working in coincidence (Fig. 1). The two plastic scintillators (NE 102 A) are optically coupled with 53 AVP photomultipliers and are protected from the light by 4 mg/cm^2 aluminium foils. The small entrance detector is 0.5 mm thick, and the larger detector is 5 cm long and has a maximum diameter of 7.5 cm. The special shape of the scintillator was chosen to optimize the light output and the solid angle, and to give as little "dead" material as possible. The dimensions of the large detector were chosen to stop about 9 MeV electrons[3)], whereas the energy loss in the small entrance detector and in the aluminium foils is about (0.10 ± 0.01) MeV for electrons in the energy range 0.5 to 20 MeV [4)].

The conversion electrons of ^{137}Cs and ^{207}Bi have been measured with and without the small detector between the source and the large scintillator, and the measured energy shift was found to be 0.103 MeV. In the following, this energy is always added to the one observed in the large scintillator.

A spectrum of conversion electrons of ^{207}Bi taken with the small detector is shown in Fig. 2. The line in Fig. 2 corresponds to the maximum energy loss of about 100 keV in the small detector. The high-energy tail of the curve is caused by electrons that are scattered in the detector. These scattered electrons are eliminated in the coincidence mode by a proper setting of a single-channel analyser, as indicated in Fig. 2 by the arrows. An electron pulse from the large detector is stored in a multichannel analyser only if there are coincideng signals from both detectors. Background from gamma radiation of the source as well as any room background is thereby suppressed. The background in on-line measuring position[1] without source is about 0.1 count per sec.

3. RESPONSE TO MONOENERGETIC ELECTRONS (POSITRONS) AND ENERGY CALIBRATION

The finite energy resolution of plastic scintillators requires a correction to the measured beta spectra. Freedman et al.[5] have described a method that takes into account the low-energy tail of a monoenergetic electron line. This method has been applied here. The measured spectrum M(E) is correlated with the true spectrum N(E) by the equation

$$M(E) = \int_{0}^{E_{max}} N(E') \, L(E,E') \, dE' \simeq \sum_{i=0}^{E_{max}} N(E_i') \, L(E_i,E_i') \, \Delta E_i' \, . \qquad (1)$$

$L(E,E')$ is the response function for monoenergetic electrons, and describes the distribution of impinging electrons of energy E' that can be detected at an energy $E \neq E'$ because of incomplete energy absorption and because of the finite resolution. $M(E)/\Delta E$ is taken as a zero-order approximation of $N(E')$. Measured line shapes have been used for $L(E,E')$. Thus one obtains a new $M_1(E)$. A first approximation to the true spectrum is given by

$$N_1(E)\,\Delta E = M(E) - [M_1(E) - M(E)] = 2M(E) - M_1(E) \, . \qquad (2)$$

By repeating this, one successively approaches the true spectrum. Two to four approximations usually give an accuracy of about 2% [5]. $N_1(E)$ is calculated by taking the average of $[M_1(E) - M(E)]$ over one full width at half maximum (FWHM) of a monoenergetic electron line at the corresponding energy. This avoids enlargements of errors due to measured points with big deviations from the continuum.

If statistical processes alone determine the response function of the scintillator, one expects the response function of monoenergetic electrons to be a Gaussian curve. The FWHM ΔE should have an energy dependence of $\Delta E \propto E^{1/2}$ [6]. Cramer et al.[7] found this relationship to be valid for monoenergetic electrons between 1 MeV and 3 MeV, whereas there exist contradictory results for conversion electrons below 1 MeV [7-11]. The response functions of monoenergetic electrons and positrons in the energy range 3.1 MeV to 9 MeV have been measured using the external beam of the Heidelberg betatron. The energy spread of the betatron beam (FWHM) is about 3% to 5% [12] and in order to obtain the resolution of the scintillator, 3% has always been quadratically subtracted from the measured width. The scintillator response for electrons and positrons of 3.1 MeV is shown in Fig. 3. On the high-energy side, the positron line shows the effect of pile-up with Compton recoil electrons from annihilation radiation. The essential part of the response function is a Gaussian-like curve, but there is a tail at the low-energy side because of back-scattering. The electron lines have been fitted with a computer program by the superposition of two Gaussian curves, where the second Gaussian curve, which was introduced to fit the tail and was cut off at the position of the main Gaussian curve, had a larger FWHM than the main curve. For positron lines, a third Gaussian line was used for fitting the pile-up effect. The result of the fits at three different energies is shown in Fig. 4. These results were used for the response function $L(E,E')$ in Eq. (1). The behaviour of the normalized resolution $\Delta E/E^{1/2}$ as a function of the energy is shown in Fig. 5. It is in agreement with the assumption $\Delta E \propto E^{1/2}$ up to 8 MeV.

Since there are no sources for conversion electrons with energies higher than 1 MeV, calibration points at higher energies can be obtained by use of beta particles of known end-point energies or by the Compton edge of high-energy gamma lines. The theoretical sharp Compton edge is in practice smeared out due to the finite energy resolution, and the remaining "peak" of the measured distribution is shifted toward lower energies[7]. Calibration points obtained from Compton recoil electrons have to be corrected for this shift. In the notation of Cramer et al.[7] the function f_p describes the fraction of the Compton-edge energy $E_{Compton}$ at which the peak of the measured distribution appears. The Klein-Nishina cross-section $K(E,\alpha)$ [13] has been folded with a Gaussian curve $G(E,E',\Delta E)$:

$$\bar{K}(\alpha,E,\Delta E) = \int_0^{E_{Compton}} K(E',\alpha)\, G(E,E',\Delta E)\, dE' \qquad (3)$$

$$f_p = \frac{\max(\bar{K})}{E_{Compton}} . \qquad (4)$$

Here $K(E,\alpha)$ is the cross-section for giving an electron a recoil energy in the interval between E and $E + dE$, and α is the energy of the gamma radiation in units of the electron rest mass. ΔE stands for the FWHM of the Gaussian curve, and $\max(\bar{K})$ is the energy of the Compton "edge" as calculated by Eq. (3). The numerical integration has been done with a procedure described by Waetzig[14]. The function f_p is shown in Fig. 6, assuming 10%, 15% and 20% FWHM of the Gaussian curve at 1 MeV. For the spectrometer described, the FWHM at 1 MeV is about 15%. The resulting energy calibration curve, including monoenergetic electrons as well as Compton recoil electrons, is shown in Fig. 7. Within the experimental accuracy (~ 2%), the relationship between pulse-height and energy is linear. The calibration curve presented here confirms the result of Cramer et al.[7], where the linearity at energies higher than 5 MeV is based on a single calibration point at 13.4 MeV.

4. INFLUENCE OF ANNIHILATION RADIATION

The different line shapes for monoenergetic electrons and positrons (Fig. 3) indicate that the amount of pile-up is not negligible. To study this effect in more detail a scintillator with the same dimensions as the large scintillator, but containing two holes of 5 mm diameter and 4.5 cm length each, was built. A source of ^{18}F of known strength was placed at different locations inside the holes in the plastic scintillator. By using an absorber for the positrons from ^{18}F, only Compton recoil electrons of annihilation radiation were recorded. Varying the position inside the scintillator simulates different positron energies. By counting the integral Compton recoil electron spectrum one obtains the detection efficiency ϵ of annihilation radiation as a function of the positron energy *). The scintillator used for this experiment and the efficiency ϵ giving the fraction of Compton recoil electrons per positron decay are shown in Fig. 8. The energy scale included in Fig. 8 is based on the range-energy relation for electrons[3)], assuming that the annihilation takes place at a position determined by the full range of a certain positron energy. This energy scale is, of course, nominal, since scattering in the scintillator has not been taken into account. The pile-up effect for this scintillator is of the order of 10%. A similar experiment was performed with a scintillator of the same diameter but twice the length, and the corresponding value of ϵ was found to be about 25% to 30%.

In order to avoid this pile-up, a method described by D'Auria and Preiss[15)] was applied. The spectrometer was sandwiched between two 6″ × 4″ NaI(Tl) crystals, and coincident signals of 511 keV from both crystals were required to store a pulse from the large plastic detector in a multichannel analyser. The influence of this coincidence arrangement on the beta end-point energy is discussed below.

5. MEASUREMENTS OF BETA SPECTRA

The spectrometer was tested by measuring some beta spectra of nuclides with known end-point energies, as listed in Table 1.

Fermi-Curie plots of the beta spectra of ^{90}Y, ^{106}Rh, and ^{68}Ga in radioactive equilibrium with ^{90}Sr, ^{106}Ru, and ^{68}Ge, respectively, are shown in Figs. 9 to 11. For the $2^- - 0^+$ transition of ^{90}Y, the shape factor of Riehs[16)] was applied.

In order to investigate the influence of the pile-up due to Compton recoil electrons of the annihilation radiation, the positron spectrum of ^{82}Rb has been measured both in the usual double coincidence and also in the fourfold coincidence mode as described in Section 4. Fermi-Curie plots of ^{82}Rb spectra are shown in Fig. 12a and 12b. The end-point energy measured

---

*) The author is grateful to Prof. P.G. Hansen, who suggested this procedure.

in fourfold coincidence (3.35 ± 0.06 MeV) is not significantly lower than in double coincidence (3.43 ± 0.05 MeV). A second component in the beta spectrum has an observed end-point energy of (2.57 ± 0.06) MeV and (2.60 ± 0.07) MeV for the two arrangements, respectively. The average energy difference of the two beta components of (0.81 ± 0.06) MeV agrees with the energy of the first excited level in ^{82}Kr of 0.777 MeV [17].

Another way of seeing the influence of Compton recoil electrons on the end-point energy of positron spectra is to use, for the same measured spectrum, the response functions of monoenergetic electrons and positrons in Eq. (1). This was done for a ^{82}Rb spectrum, and again the same end-point energies within the experimental errors were found. This leads to the conclusion that the influence of Compton recoil electrons to positron end-point energies is small. Therefore, also positron spectra can be measured in the double coincidence arrangement.

A study was made of ^{118}I as a first application of the spectrometer for beta energy measurements of samples produced at the ISOLDE on-line mass separator. Six-minute ^{118}Xe was collected for 20 min and allowed to decay for 40 min to remove the xenon activity. Positron spectra of 14.3 min ^{118}I were measured. Also in this case the double and the fourfold coincidences gave the same result within the experimental error. A Fermi-Curie plot of a ^{118}I spectrum is shown in Fig. 13. The end-point energy was found to be (5.27 ± 0.29) MeV. Only two measurements of the ^{118}I beta spectrum could be found in the literature. Andersson et al.[18] measured mass-separated ^{118}I by absorption techniques and reported a Q-value of about 8 MeV, which corresponds to about 7 MeV positron end-point energy, provided the transition leads to the ground state. Butement and Qaim[19] found that ^{118}I emits positrons of 5.5 MeV end-point energy. In the work of Butement and Qaim the mass assignment was based on mass formula calculations.

6. CONCLUSION

Applying corrections for the measured spectra, the beta end-point energies obtained in this work compare favourably with measurements of magnetic spectrometers. Therefore with this scintillation spectrometer one can expect to obtain maximum beta energies of short-lived isotopes with an accuracy of about 5%. Of course, the experimental accuracy might be limited by several facts, i.e. a complicated beta continuum or the low activity of the sources.

Acknowledgements

The author wishes to express his gratitude to Prof. W. Gentner for his continuous interest and support. Thanks are due to Dr. A. Kjelberg for the hospitality given by the Nuclear Chemistry Group at CERN, Dr. G. Rudstam for many helpful discussions on data analysis, Mrs. R. Mohr and Dr. J. Alstad for the preparation of ^{18}F sources, Messrs. H.-J. Dahmen and F. Dreyer for the use of the Heidelberg betatron, Dr. F. Münnich for helpful discussions, and Mr. W. Waetzig for the use of an Algol-program. Last but not least, my grateful acknowledgements go to Dr. J. Jastrzebski, who participated in the early stages of the work and who gave me much useful advice.

Table 1

Isotope	Type of decay	E_{max} (MeV) Present work	Literature †)	Ref.
^{90}Y	β^-	2.29 ± 0.03	2.268 ± 0.002	a
			2.271 ± 0.002	b
			2.284 ± 0.005	c
			2.273 ± 0.005	d
^{106}Rh	β^-	3.52 ± 0.12	3.53 ± 0.01	e
			3.55	f
			3.55 ± 0.01	g
^{68}Ga	β^+	1.97 ± 0.10	1.88 ± 0.02	h
			1.94 ± 0.05	i
			1.88 ± 0.02	j
^{82}Rb	β^+	3.35 ± 0.06	3.15 ± 0.03	k
			3.5	m **)
^{118}I	β^+	5.27 ± 0.29	~7	n **)
			5.5	o *)

†) The listed literature values include measurements with magnetic spectrometers and scintillation spectrometers (*) and with absorption techniques (**).

a) S. Andre and P. Depommier, J. Phys. (Paris) 25, 673 (1964).

b) R.T. Nichols, R.E. McAdams and E.N. Jensen, Phys.Rev. 122, 172 (1961).

c) H. Daniel, G.Th. Kaschl, H. Schmitt and K. Springer, Phys.Rev. 136 B, 1240 (1964).

d) L.M. Langer, E.H. Spejewski and D.E. Wortman, Phys.Rev. 135 B, 581 (1964).

e) D.E. Alburger, Phys.Rev. 88, 339 (1952).

f) S.Y. Ambiye and R.P. Sharma, Nuclear Phys. 29, 657 (1962).

g) E.P. Grigorev, A.V. Zolotavin, I.I. Kuzmin and E.D. Pavlitskaia, Izv.Akad.Nauk SSSR, Ser.Fiz. 22, 194 (1958) [translation: Bull.Acad.Sci. USSR, Phys.Ser. 22, 191 (1958)].

h) A. Mukerji and P. Preiswerk, Helv.Phys.Acta 25, 387 (1952).

i) B. Craseman, D.E. Rehfuss and H.T. Easterday, Phys.Rev. 102, 1344 (1956).

j) H. Daniel, Z.Naturforsch. 12 A, 363 (1957).

k) S.V. Castner and D.H. Templeton, Phys.Rev. 88, 1126 (1952).

m) B.V. Kurchatov, V.N. Mekhedov, N.I. Borisova, M.Ya. Kuznetsova, L.N. Kurchatova and L.V. Christyakov, Conf.Acad.Sci. on the Peaceful Uses of Atomic Energy, Chem.Sci., p. 178 (1958); Consultants Bureau Transl. p. 111.

n) See Ref. 18).

o) See Ref. 19).

REFERENCES

1) "The ISOLDE on-line isotope separator facility at CERN", to be published as a CERN Yellow report.

2) I. Amarel, R. Bernas, R. Foucher, J. Jastrzebski, A. Johnson, J. Teillac and H. Gauvin, Phys. Letters 24 B, 402 (1967).

3) R.D. Birkhoff in Handbuch der Physik XXXIV (S. Fluegge, Ed.) (Springer-Verlag, Berlin-Göttingen-Heidelberg, 1958), p. 70.

4) B. Marion, 1960 Nuclear Data Tables (USAEC, 1960), p. 7.

5) M.S. Freedman, T.B. Novey, F.T. Porter and F. Wagner, Jr., Rev.Sci. Instrum. 27, 716 (1965).

6) J.B. Birks, The theory and practice of scintillation counting (Macmillan, New York, 1964), p. 370.

7) J.G. Cramer, Jr., B.J. Farmer and C.M. Class, Nuclear Instrum. Methods 16, 289 (1962).

8) H.E. Bosch and T. Urstein, Nuclear Instrum. Methods 24, 109 (1963).

9) T.J. Kennett and G.L. Keech, Nuclear Instrum. Methods 24, 142 (1963).

10) B. Persson, Nuclear Instrum. Methods 27, 1 (1964).

11) D.L. Smith, R.G. Polk and T.G. Miller, Nuclear Instrum. Methods 64, 157 (1968).

12) F. Dreyer, private communication.

13) Ch. Davisson, Alpha-, beta- and gamma-ray spectroscopy (K. Siegbahn, Ed.) (North-Holland Publishing Co., Amsterdam, 1965), p. 54.

14) W. Waetzig, Diplomarbeit (Braunschweig, 1966), unpublished.

15) J.M. D'Auria and I.L. Preiss, Nuclear Phys. 84, 37 (1966).

16) P. Riehs, Nuclear Phys. 75, 381 (1966).

17) C.M. Lederer, J.M. Hollander, I. Perlman, Tables of Isotopes (Wiley and Sons, New York, London, Sydney, 1967).

18) G. Andersson, G. Rudstam and G. Sørensen, Ark.Fys. 28, 37 (1964).

19) F.D.S. Butement and S.M. Qaim, J.Inorg.Nucl.Chem. 27, 1729 (1965).

Figure captions

Fig. 1 : Schematic diagram of the spectrometer.

Fig. 2 : The conversion electron spectrum of ^{207}Bi taken with the small detector. The arrows indicate the settings of a single-channel analyser for the coincidence mode.

Fig. 3 : Line shapes for electrons (lower part) and positrons (upper part) for 3.1 MeV betatron energy.

Fig. 4 : Positron lines measured at different betatron energies. The solid curves are fits obtained by superposition of three Gaussian curves.

Fig. 5 : $\Delta E/E^{1/2}$ for the energy range 1 MeV to 9 MeV. The point at 976 keV was obtained using a ^{207}Bi source, the others by monoenergetic electrons from a betatron. Full circles are used for electrons and open ones for positrons. The curve is normalized to 1 at 3 MeV.

Fig. 6 : Upper part: the function f_p calculated for an assumed resolution of the scintillator (FWHM) of 10%, 15% and 20% at 1 MeV.

Lower part: the result of folding the Klein-Nishina cross-section with a Gaussian curve of 15% FWHM at 1 MeV. E_c is the energy of the theoretical sharp Compton edge.

Fig. 7 : Energy calibration curve obtained by the use of monoenergetic electrons from a betatron (full circles) and Compton recoil electrons (open circles).

Fig. 8 : The fraction ϵ of Compton recoil electrons from annihilation radiation detected per positron decay as a function of the positron energy (see the text about the energy scale). The lower part shows the shape of the scintillator used for the determination of ϵ.

Fig. 9 : Fermi-Curie plot of a ^{90}Y electron spectrum.

Fig. 10 : Fermi-Curie plot of a ^{106}Rh electron spectrum.

Fig. 11 : Fermi-Curie plot of a ^{68}Ga positron spectrum.

Fig. 12 : Fermi-Curie plot of a ^{82}Rb spectrum taken (a) in fourfold coincidence and (b) in double coincidence. Two components were found.

Fig. 13 : Fermi-Curie plot of a ^{118}I positron spectrum.

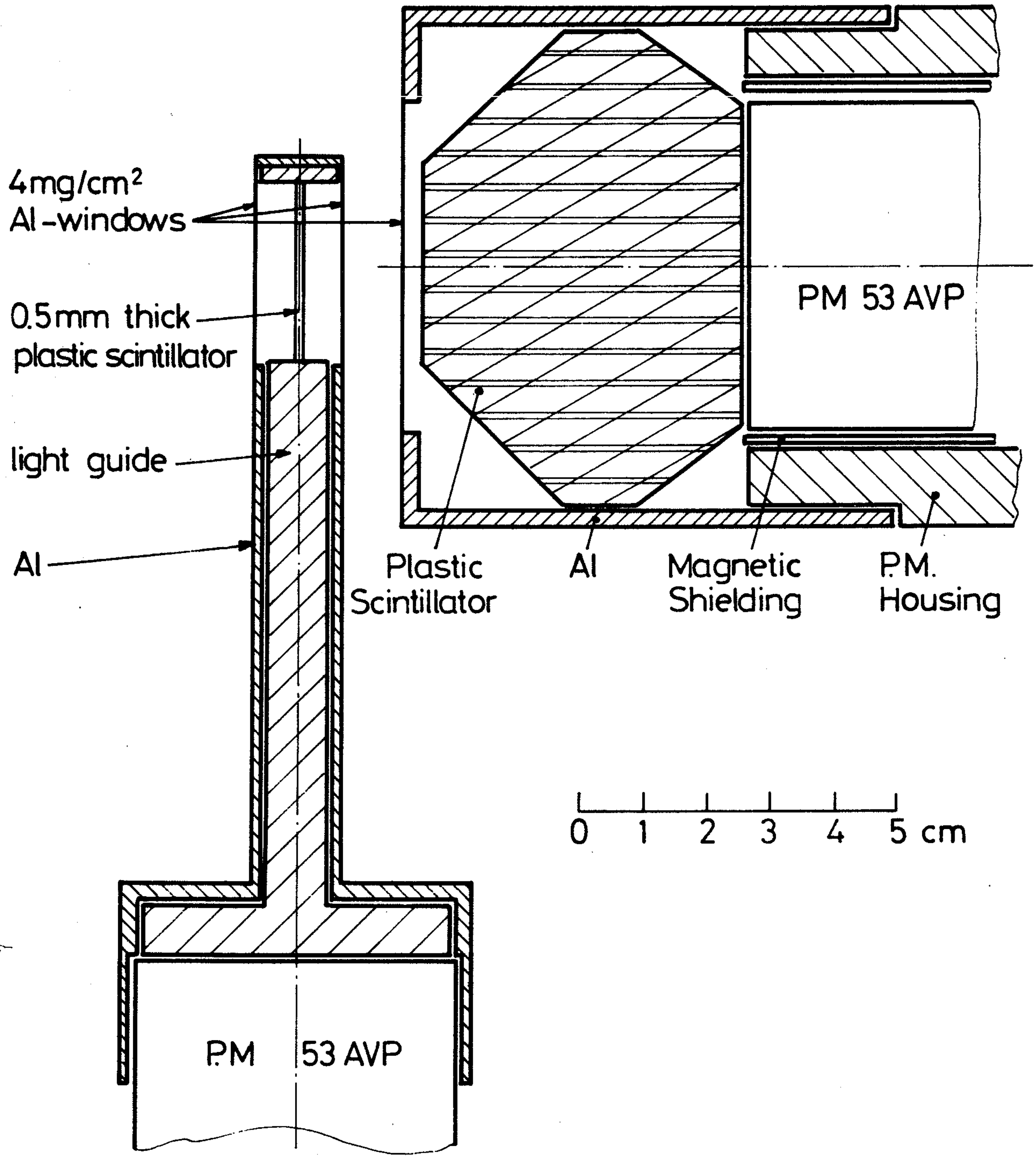
4mg/cm²
Al-windows
0.5mm thick
plastic scintillator
light guide
Al
P.M 53 AVP
PM 53 AVP
Plastic
Scintillator
Al
Magnetic
Shielding
P.M.
Housing
0 1 2 3 4 5 cm

Fig. 1

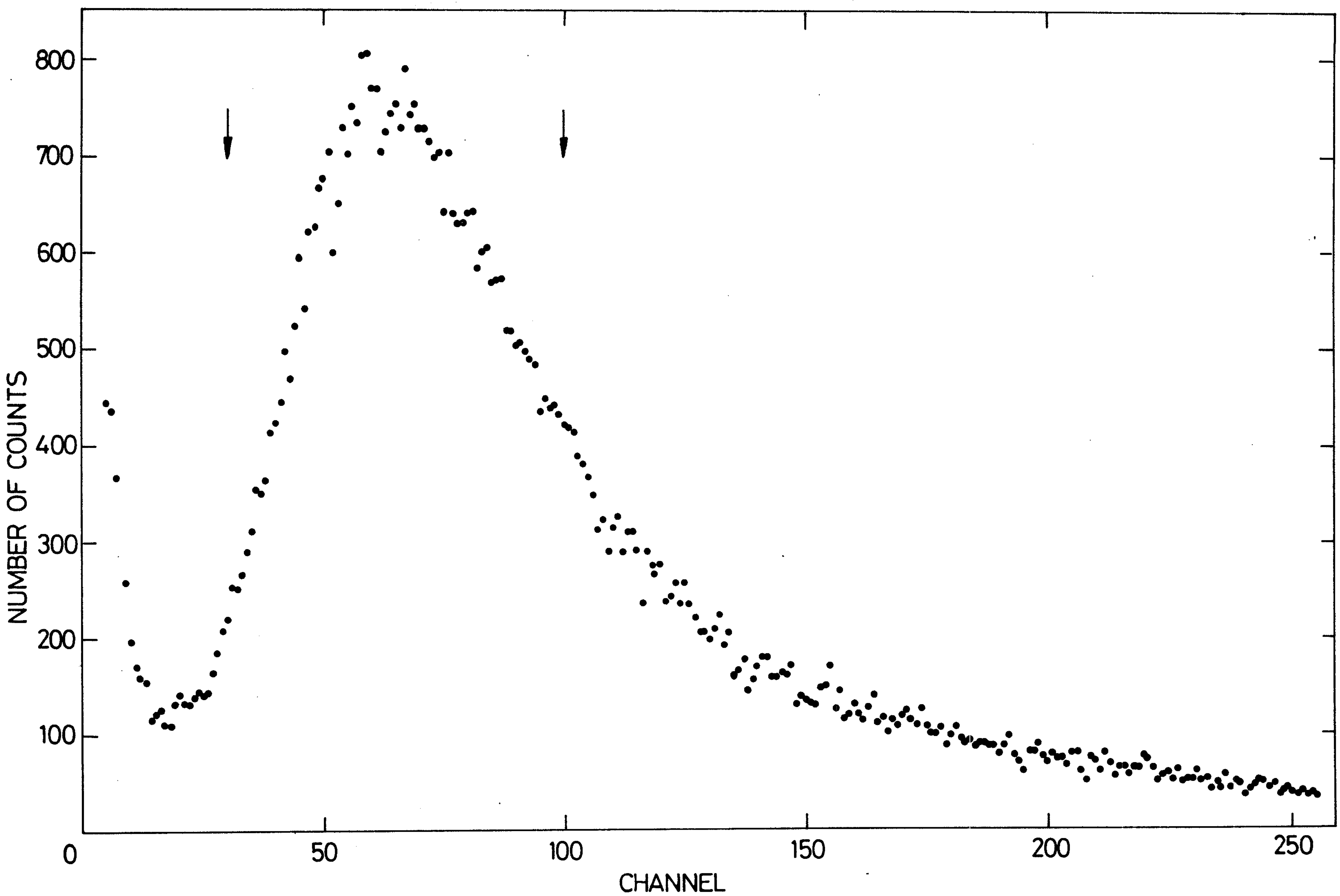
800
700
600
500
400
300
200
100
NUMBER OF COUNTS
0
50
100
150
200
250
CHANNEL

Fig. 2

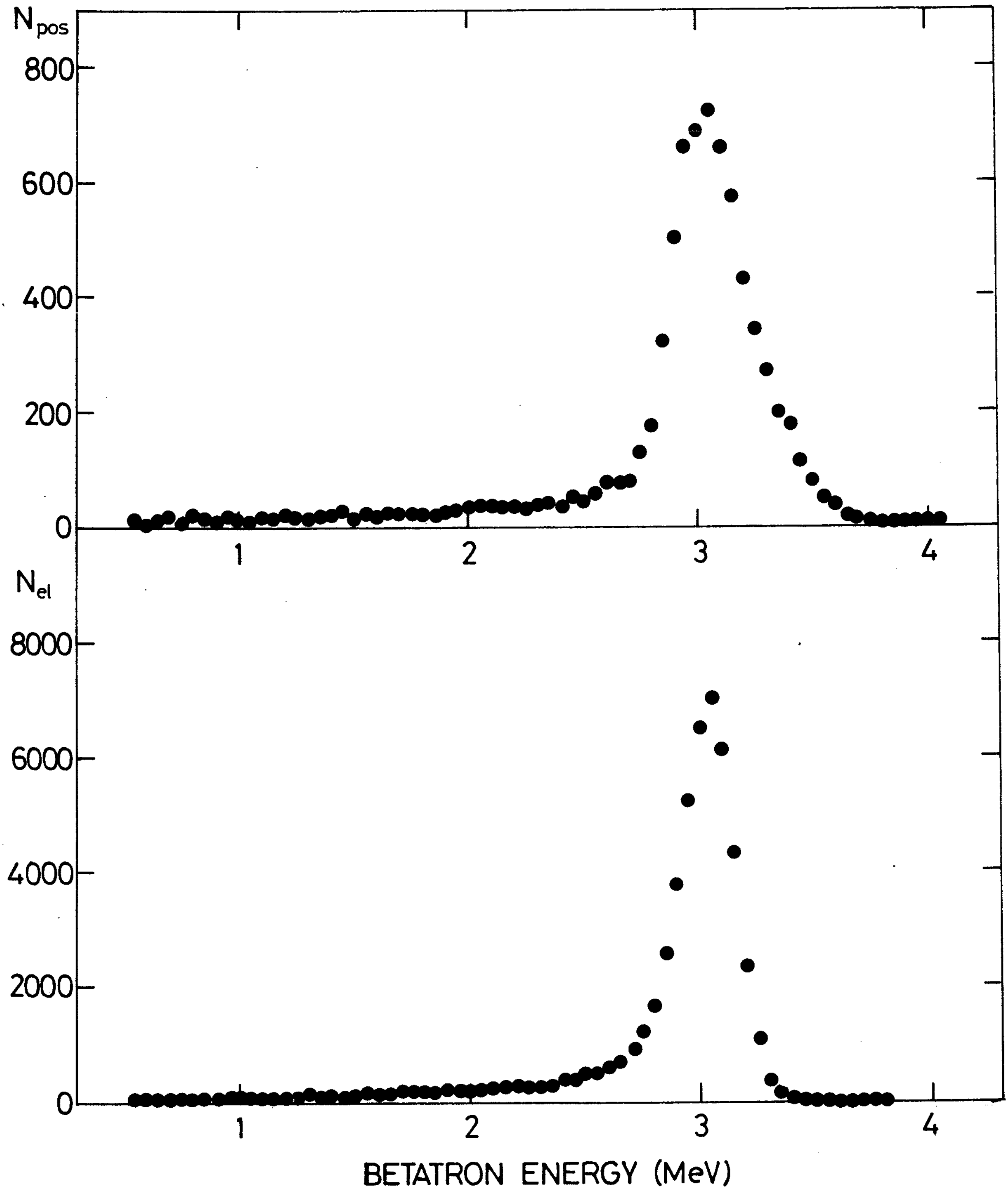
N pos
800
600
400
200
0
1
2
3
4
N el
8000
6000
4000
2000
0
1
2
3
4
BETATRON ENERGY (MeV)

Fig. 3

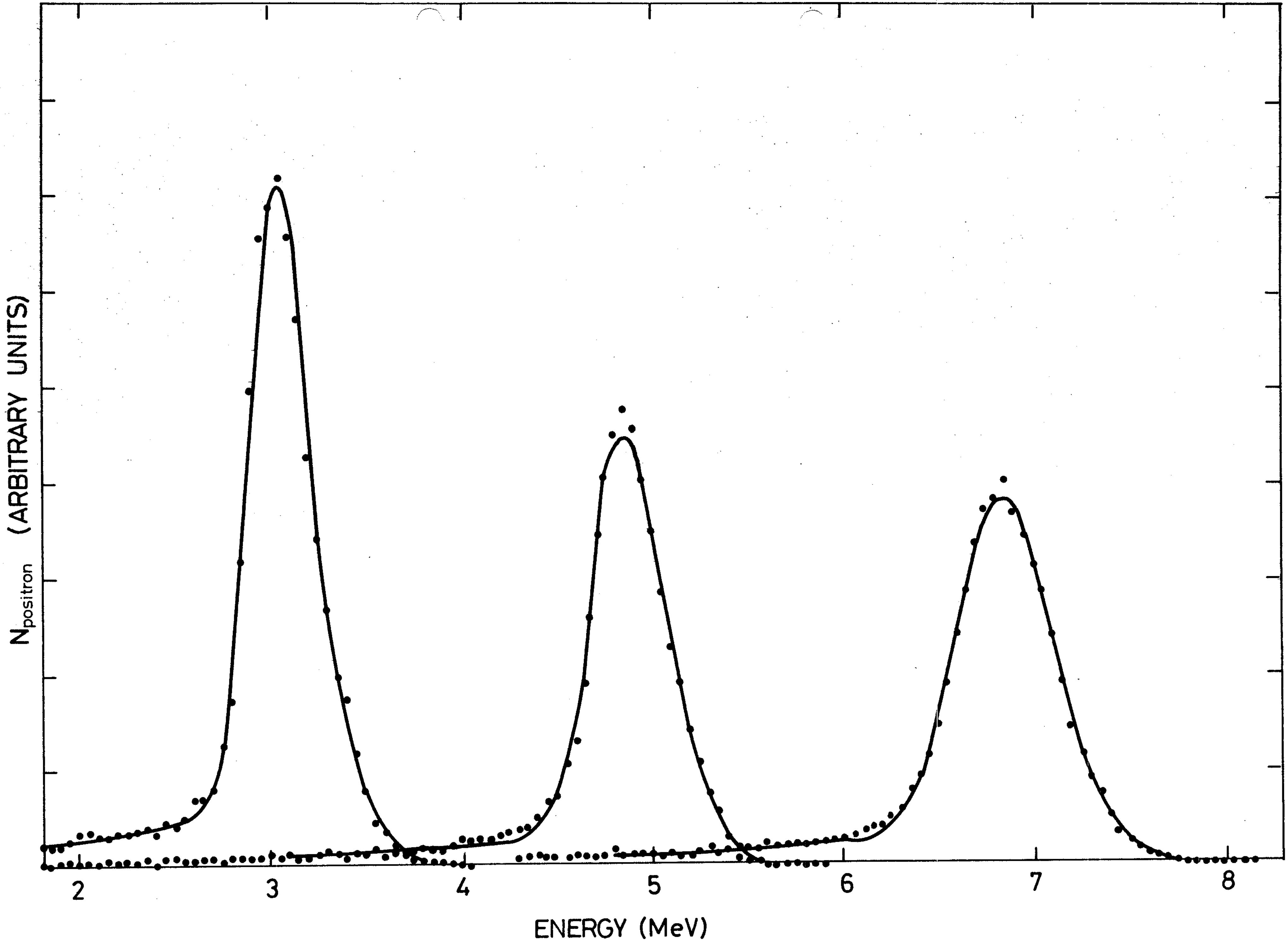

Fig. 4

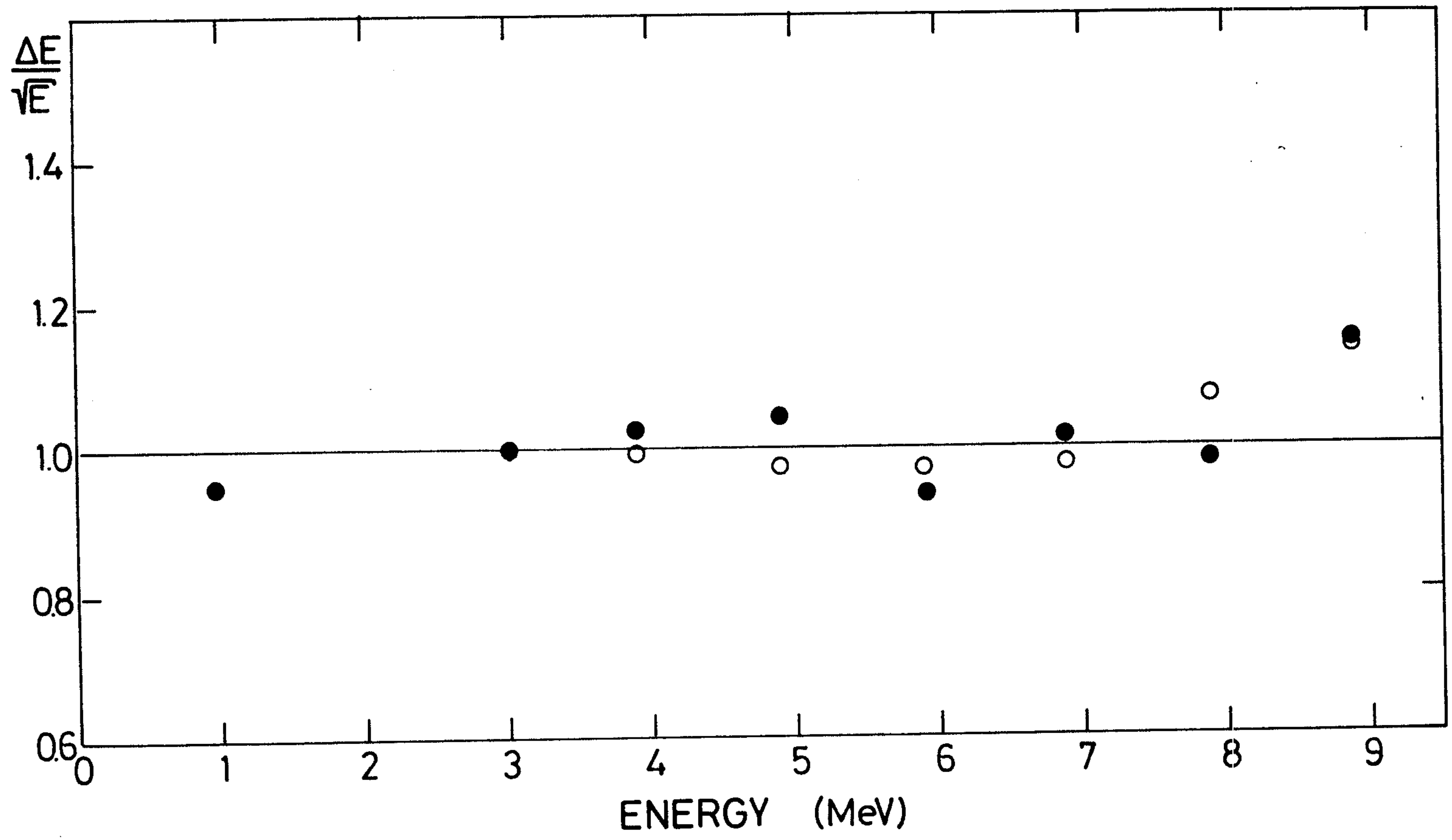

Fig. 5

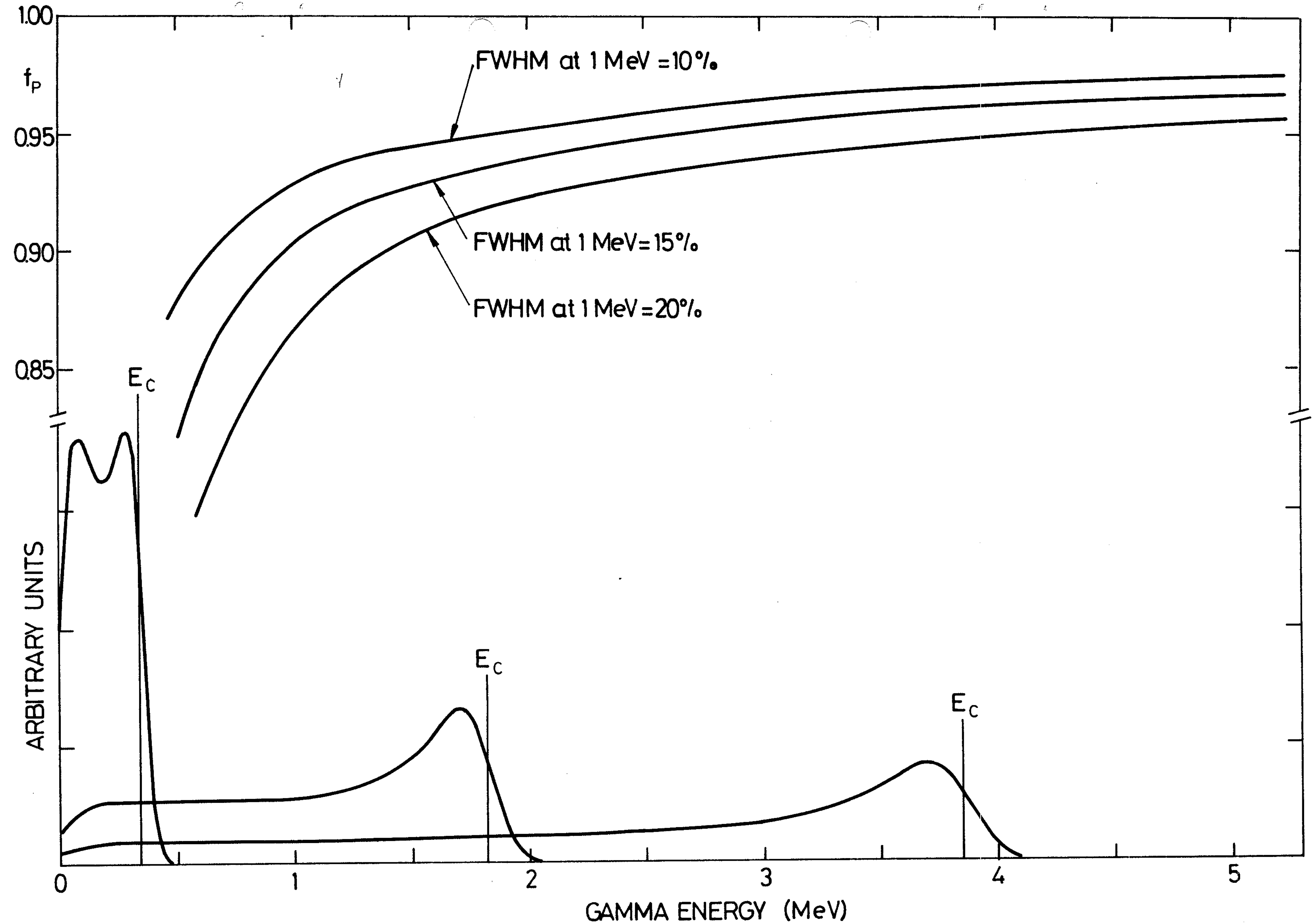
1.00
f_P
0.95
0.90
0.85
FWHM at 1 MeV =10%
FWHM at 1 MeV=15%
FWHM at 1 MeV=20%
E_C
E_C
E_C
ARBITRARY UNITS
0
1
2
3
4
5
GAMMA ENERGY (MeV)

Fig. 6

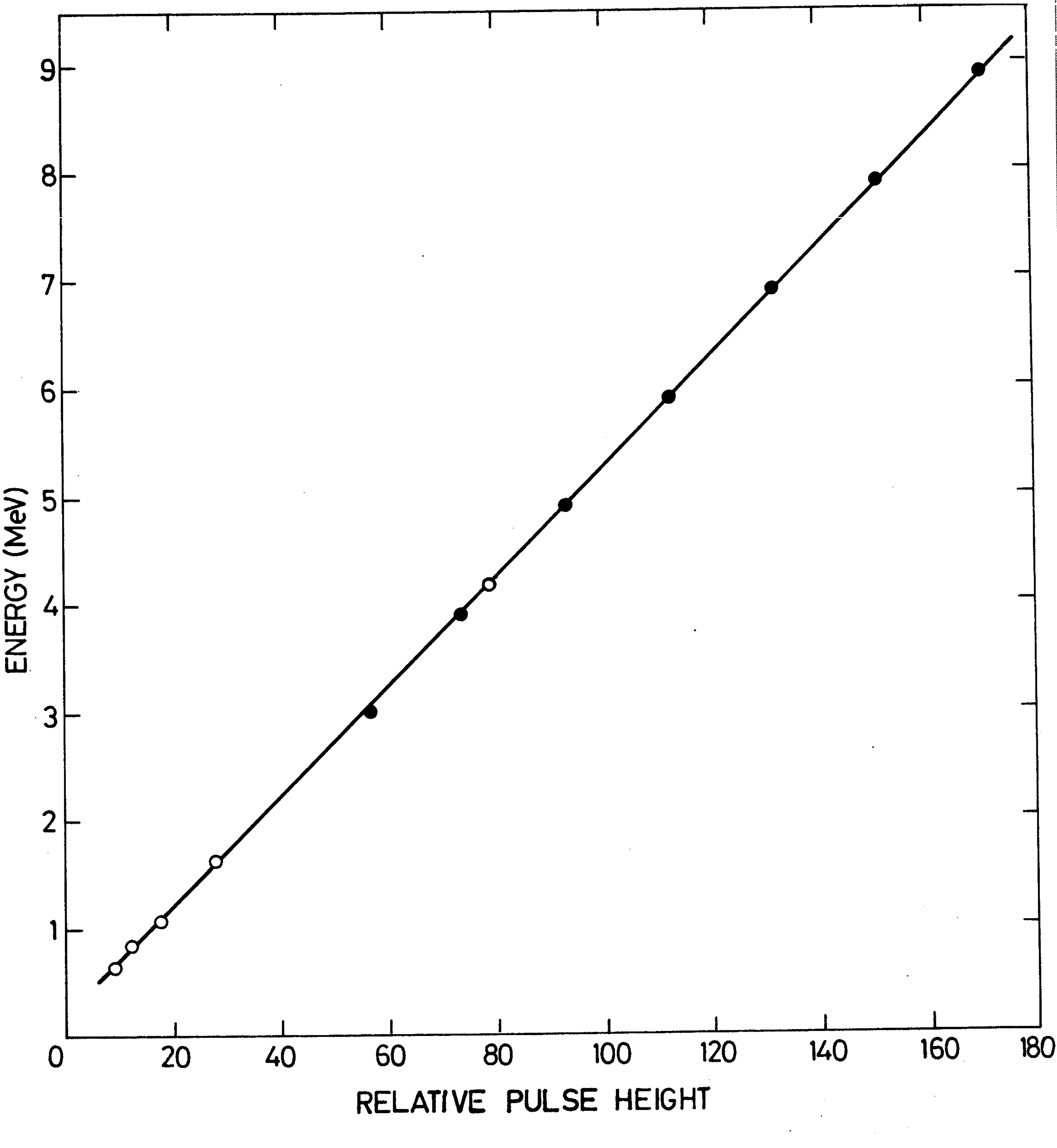

ENERGY (MeV)
9
8
7
6
5
4
3
2
1
0
20
40
60
80
100
120
140
160
180
RELATIVE PULSE HEIGHT

Fig. 7

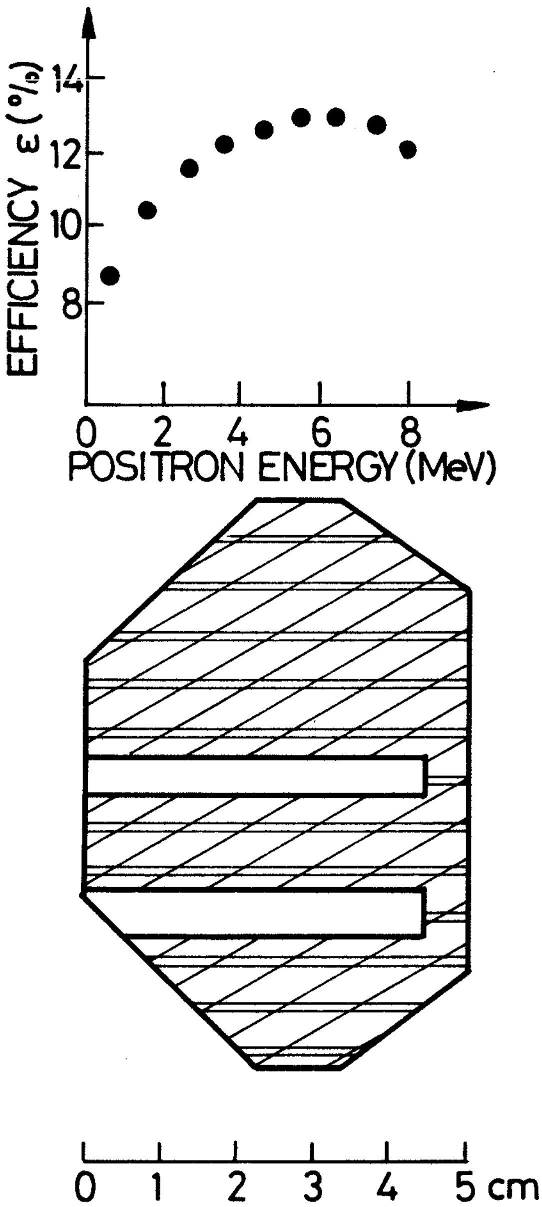

Fig. 8

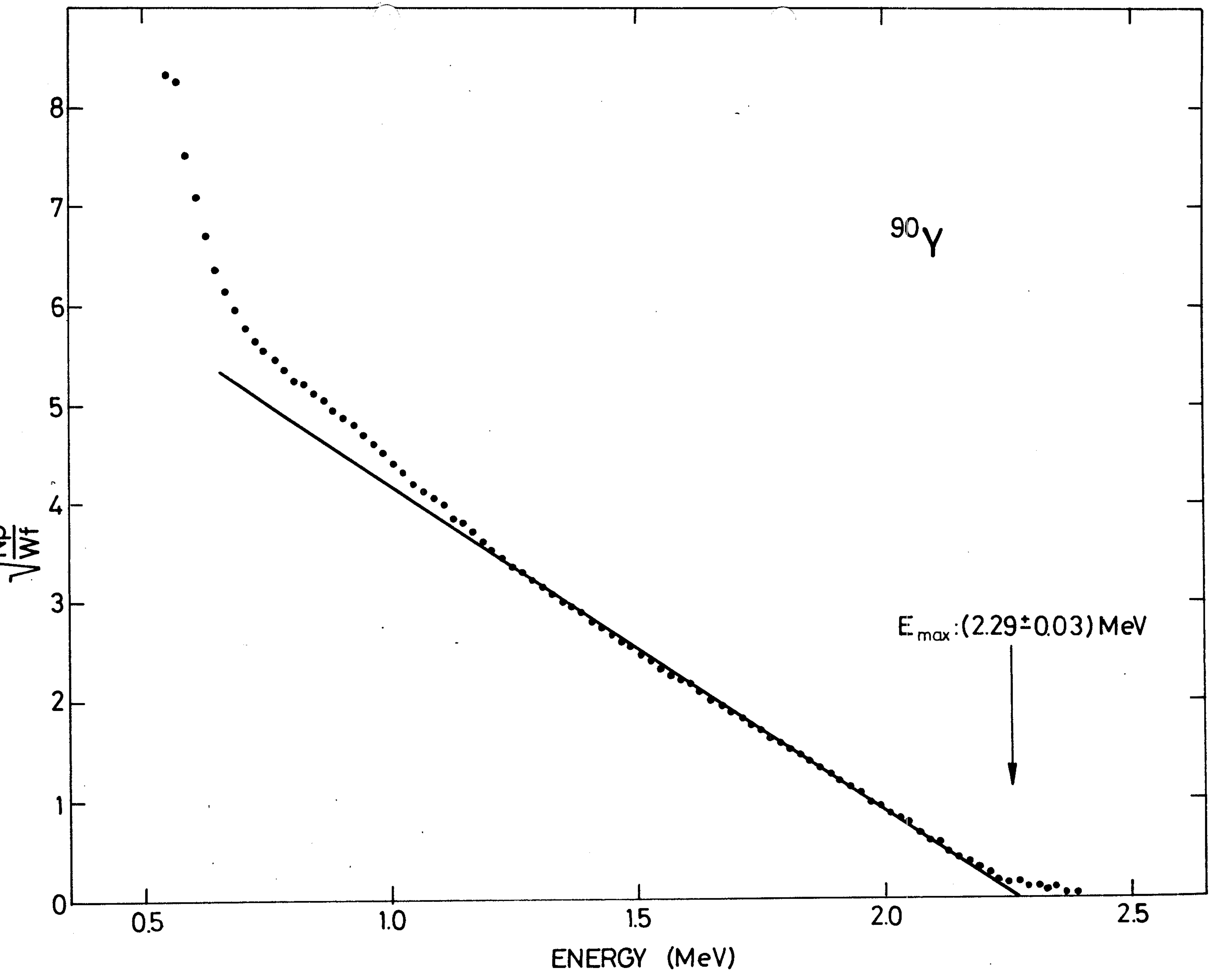

^{90}Y
E_{max}:(2.29±0.03) MeV
$\sqrt{\frac{Np}{Wf}}$
0
1
2
3
4
5
6
7
8
0.5
1.0
1.5
2.0
2.5
ENERGY (MeV)

Fig. 9

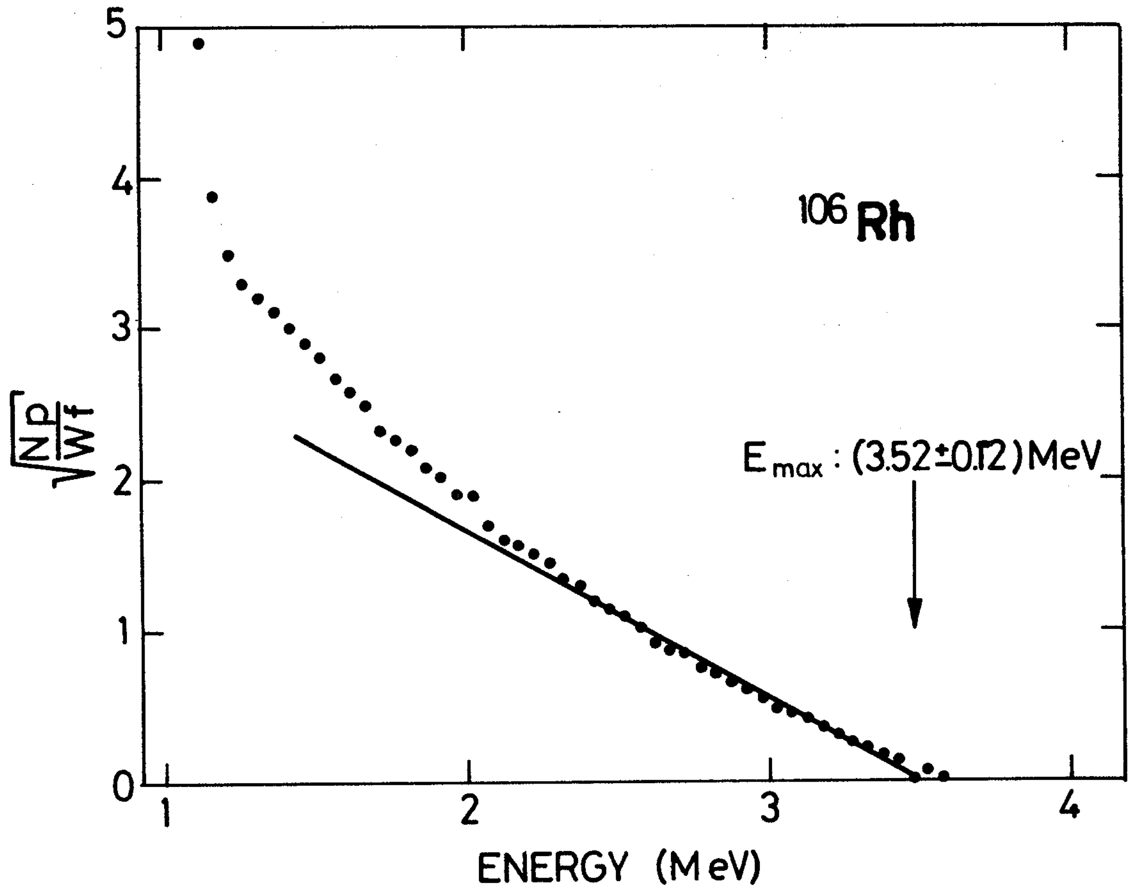

Fig. 10

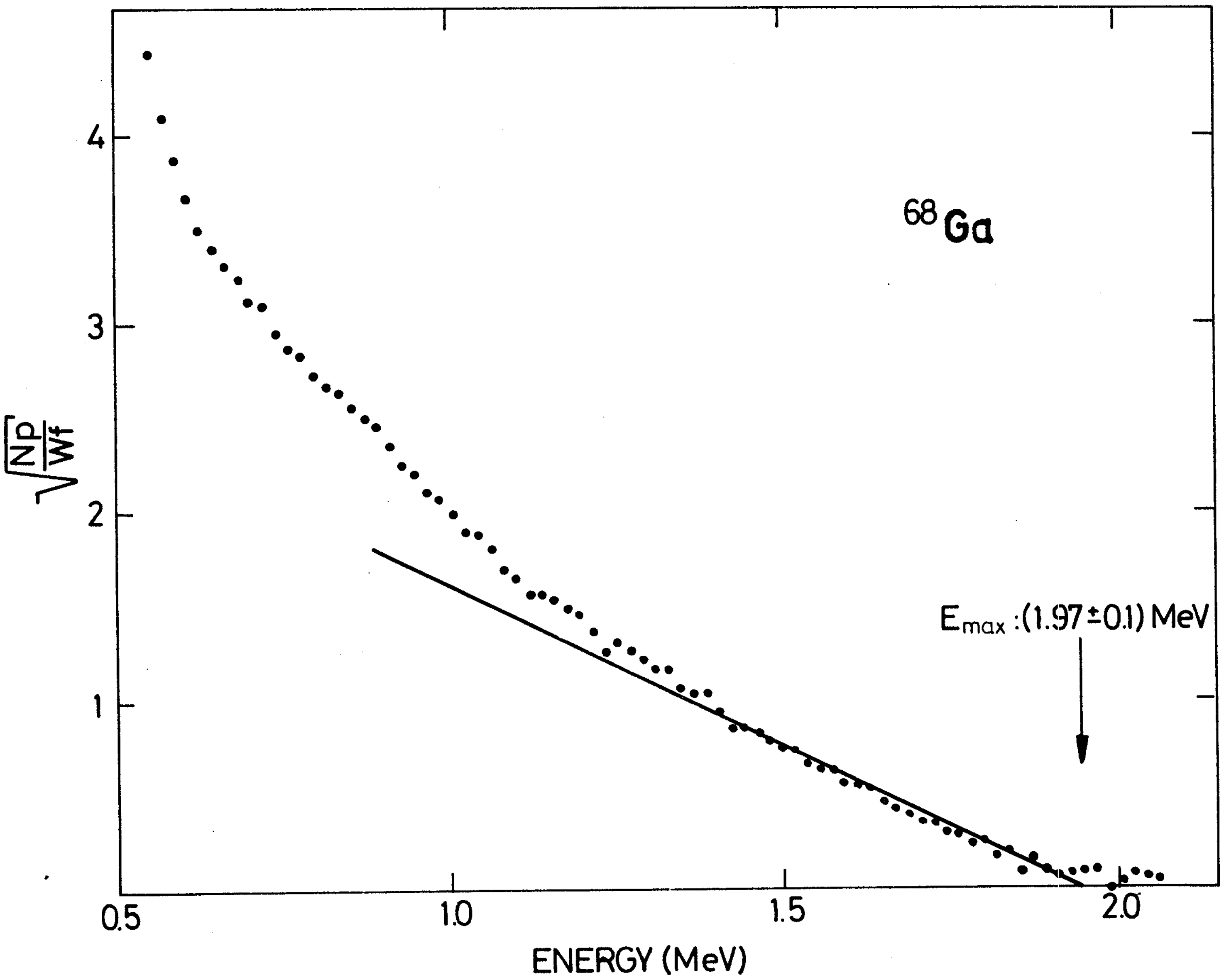

Fig. 11

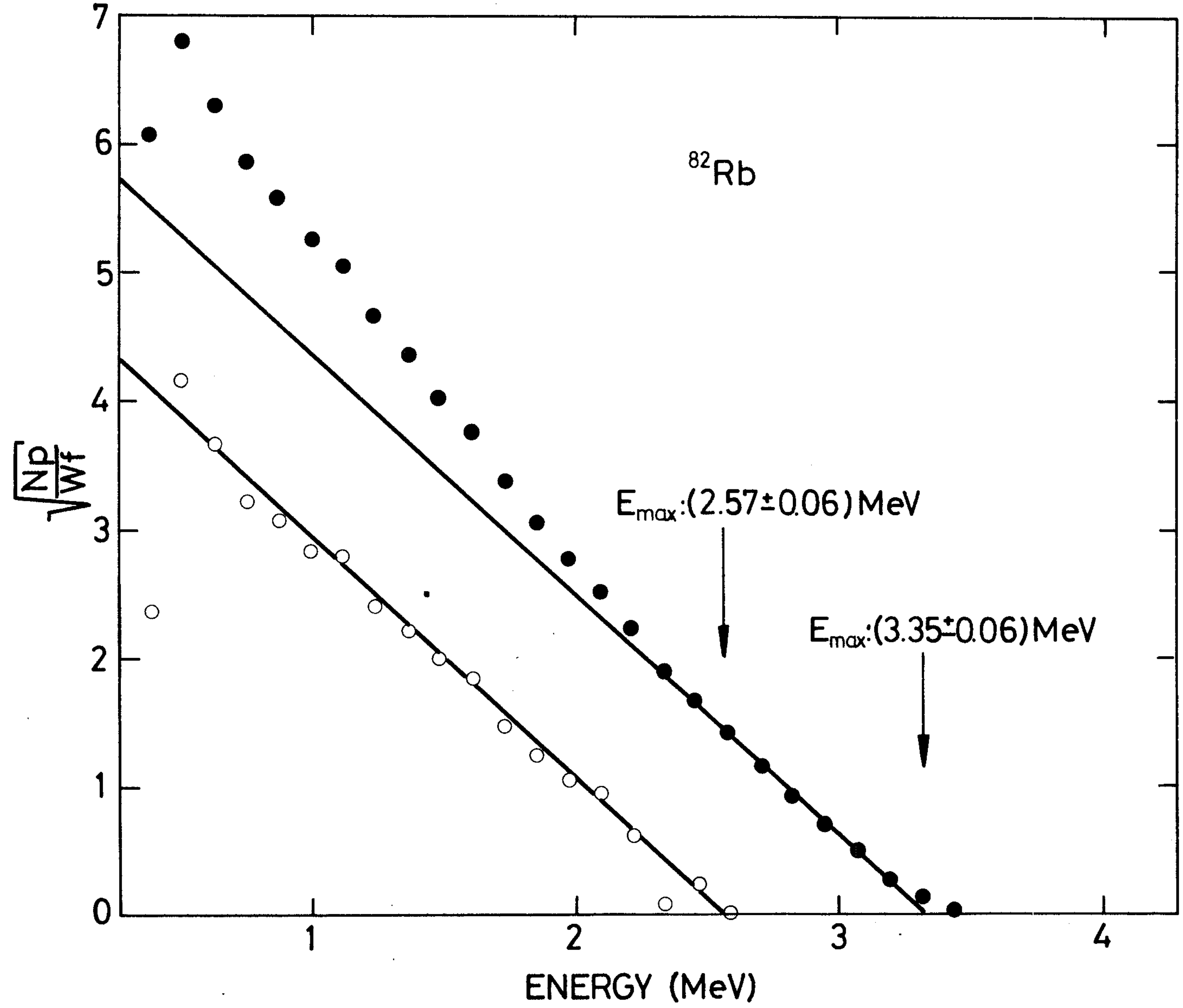

Fig. 12a

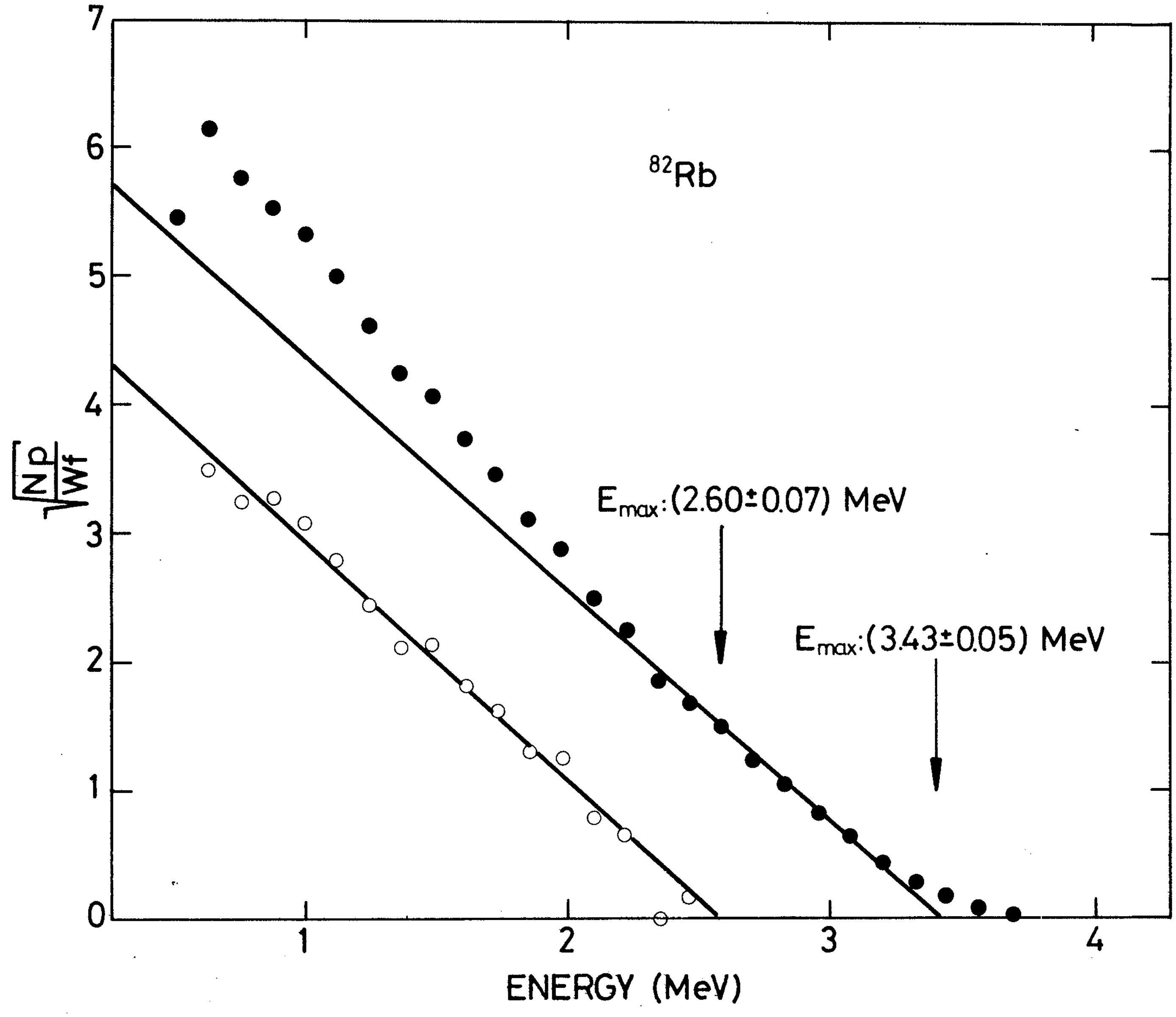

82Rb
Emax:(2.60±0.07) MeV
Emax:(3.43±0.05) MeV
ENERGY (MeV)
√(Np/Wf)
0
1
2
3
4
5
6
7

Fig. 12b

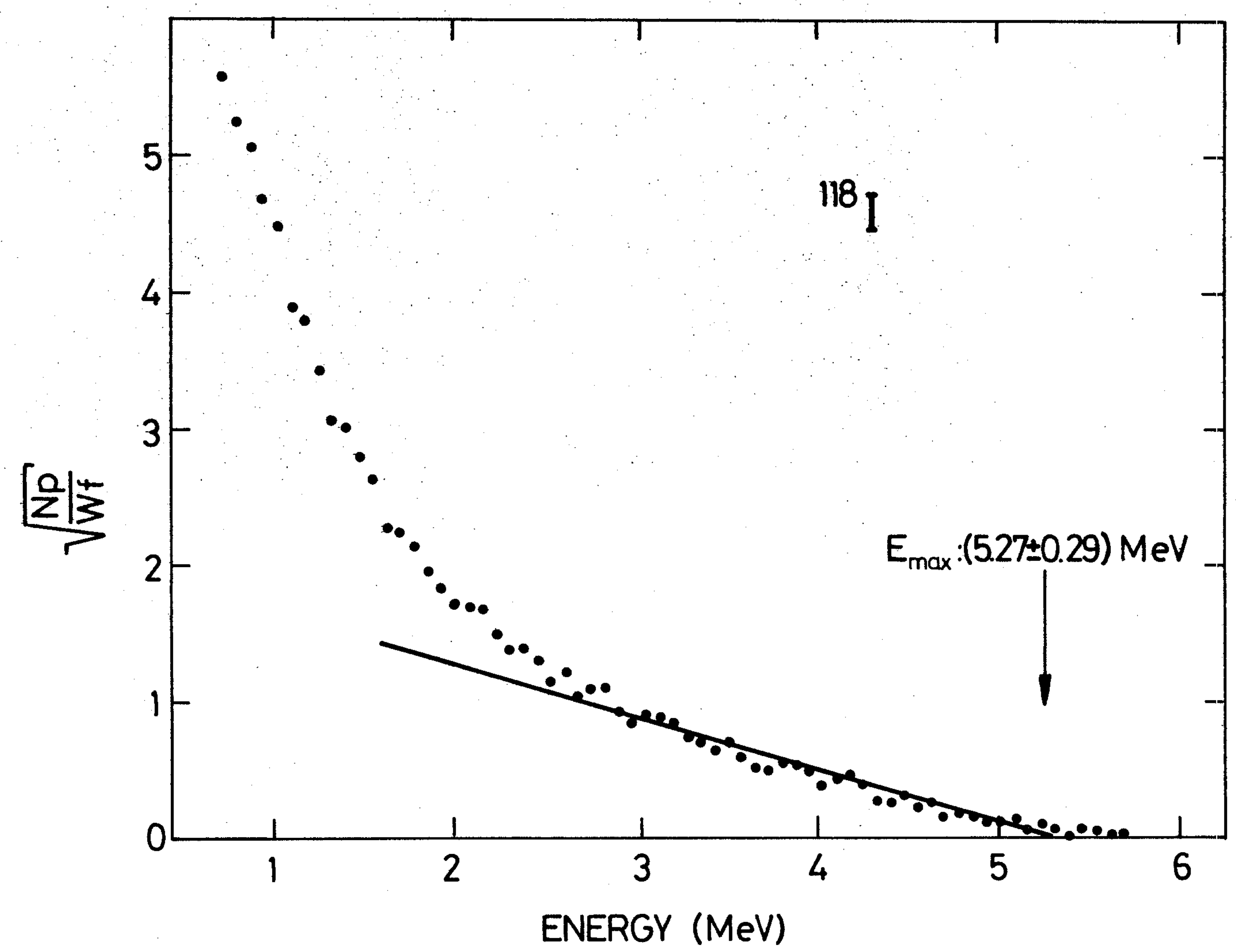

Fig. 13